

Jets in Active Galaxies

D J Saikia

Jets in active galaxies are signatures of energy supply via collimated beams of plasma from the galactic nucleus to the extended regions of emission. These jets, which occur across the electromagnetic spectrum, are powered by supermassive black holes in the centres of the host galaxies. Jets are seen on the scale of parsecs in the nuclear regions to those which power the giant radio sources extending over several megaparsecs. These jets raise many challenging astrophysical questions. This article explores some aspects of jets in radio galaxies and quasars, which are amongst the most powerful active galaxies.

1. Introduction

Astrophysical jets, which appear as extended, collimated structures, are believed to be caused by outflows from compact objects. These are seen in a variety of situations. These include (i) young stars and protostars, which become stars once the thermonuclear reactions in the stellar interiors start off; (ii) active galactic nuclei (AGN) associated with supermassive black holes (SMBHs) which are located in the centres of galaxies and have masses ranging from about 10^7 to $10^{10} M_{\odot}$ where M_{\odot} denotes the mass of the Sun; (iii) binary stellar systems emitting at X-ray wavelengths where a collapsed or 'dead' star, such as a white dwarf, neutron star or black hole, accretes matter from its normal stellar companion; (iv) Gamma-ray bursts which are highly energetic and catastrophic events associated with the collapse of massive stars where jets may be directed towards us; and (v) jets from pulsars, which are rapidly rotating neutron stars emitting narrow beams of radiation. Images of some of these jets are shown in *Figure 1*.

Although the term jet indicates continuous or quasi-continuous



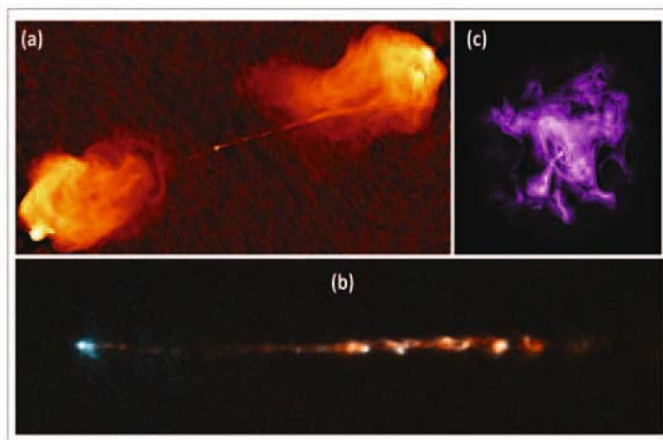
D J Saikia has been engaged in research and teaching for over forty years at the National Centre for Radio Astrophysics of the Tata Institute of Fundamental Research. He was the founding Vice-Chancellor of Cotton University at Guwahati. His research interests have been largely on extragalactic astronomy, and more recently on education and related policy issues, with an emphasis on higher education.

Keywords

Astrophysical jets, radio galaxies, quasars, supermassive black holes, radiation processes, superluminal motion, unified schemes.



Figure 1. (a) A radio image of the radio galaxy Cygnus A about 250 Mpc away made using the Very Large Array by Perley, Carilli & Dreher (Image courtesy of NRAO/AUI; <http://images.nrao.edu/AGN/>) showing the jet and a weaker counter-jet; (b) A Hubble Space Telescope image of HH34 showing the jet at optical wavelengths emanating from a protostar in Orion (<http://hubblesite.org/image/2870/gallery>; image courtesy NASA, ESA, and P Hartigan); (c) An X-ray jet observed with the Chandra X-ray Observatory in the Crab Nebula (M1, NGC1952), a supernova remnant at a distance of about 6500 light year which has a pulsar with a period of 33 millisecond (<http://hubblesite.org/image/4030/gallery>; image credit: CXC).



fluid outflows and is widely used for narrow, collimated features, hard evidences of outflows are limited. These come from either monitoring the motion of knots or compact, high-brightness regions of emission in the jets via high-resolution, milli-arcsec scale observations as in the case of jets in AGN, or from Doppler shifts of spectral lines as in the X-ray binary system SS433. In this article, we focus on powerful jets associated with radio galaxies and quasars, which belong to the broad category of active galaxies. A ‘normal’ galaxy can be described largely by the evolution of its stellar population, and its integrated spectrum is dominated by the stellar absorption lines. Active galaxies could be broadly categorized into starburst galaxies and AGN powered by SMBHs. The former exhibit intense bursts of star formation, often with star formation rates (SFR) several orders of magnitude larger than that of our Milky Way ($\text{SFR} \sim 1\text{--}2 M_{\odot} \text{ yr}^{-1}$). AGN may exhibit several exotic phenomena such as powerful emission at radio and higher frequencies, jets which can extend up to several Mpc (1 pc = 3.26 light years), prominent emission lines, and variability in both its continuum and line emission. We will examine briefly some aspects of these jets.



2. A Bit of History

In the extragalactic context, while studying optical counterparts of radio sources Baade and Minkowski in 1954 noted a “straight jet, extending from the nucleus” of the elliptical galaxy NGC 4486 (M87), which is associated with the strong radio source Virgo A (3C274), then called RYLE 12.01 and MILLS 12+1 based on early surveys. Baade and Minkowski noted that “several strong condensations are in the outer parts of the jet, which extends about 20'' from the nucleus” and that “the jet has a continuous spectrum, indicating a rather blue color but showing neither absorption nor emission lines.” Although this feature was first seen in 1918 by H Curtis of the famous Curtis–Shapley debate on the nature of ‘spiral nebulae’ and the ‘scale of the Universe’, Baade and Minkowski introduced the word *jet* into the extragalactic literature. They also noted the relative blue-shift of the centroid of the [O II] λ 3727 emission line relative to the systemic velocity¹ of the galaxy. They suggested that the “jet was formed by ejection from the nucleus” and “that the [O II] line is emitted by a part of the material which forms the jet and is still very close to, if not still inside, the nucleus.” Similarly, the ‘optical wisp’ in the first quasar to be discovered – 3C273 – which resembled the one in M87, was also referred to as a jet by Maarten Schmidt in 1963, who realized that the strong emission lines of 3C273 were the redshifted Balmer lines giving a redshift² of 0.158 (implying a luminosity distance of about 760 Mpc).

Besides Virgo A, one of the early radio sources to be identified was Cygnus A which was observed by Grote Reber in 1939. A better determination of its position by interferometric observations by Graham Smith in 1951 soon led to a reliable identification with an elliptical galaxy at a redshift of 0.056 by Dewhirst and Baade and Minkowski (implying a luminosity distance of about 250 Mpc). Almost immediately afterwards, Jennison and Das Gupta showed that the radio emission is from two lobes on either side of the optical galaxy. Better images followed with the Cambridge One Mile Telescope by Mitton and Ryle in 1969 and the Cambridge 5-km telescope by Hargrave and Ryle in 1974

The ‘optical wisp’ in the first quasar to be discovered – 3C273 – which resembled the one in M87, was also referred to as a jet by Maarten Schmidt in 1963, who realized that the strong emission lines of 3C273 were the redshifted Balmer lines giving a redshift of 0.158

¹The systemic velocity of a galaxy is due to the expansion of the Universe, and a velocity component or ‘peculiar velocity’ due to local dynamics as galaxies are usually in groups or clusters.

²Redshift is defined as $\Delta\lambda/\lambda_e$ where λ_e is the rest-frame wavelength.



which revealed bright hot-spots or intense regions of emission at the outer extremities of the lobes, and a compact radio source associated with the optical galaxy. The hotspots are identified with the regions where jets or beams of plasma interact with the external medium, dissipating energy, as it ploughs its way forward. Some of the best available images of Cygnus A have been made using the Very Large Array by Perley and his collaborators (*Figure 1*). On the theoretical front, Rees, Longair, Ryle, Scheuer, and Blandford developed some of the early models for the continuous supply of energy from the nucleus of the host galaxy to the outer lobes via channels which are seen as radio jets.

Extensive high-quality imaging of these jets at radio frequencies in the 1980s and 1990s from the parsec-scale nuclear jets to those that are hundreds of kpc long was followed by the exciting development of imaging dozens of radio jets at X-ray wavelengths. This was possible with the launching of the Chandra X-ray Observatory in 1999 which had high resolution and sensitivity. Multi-wavelength observations facilitated exploring several questions related to the physics of jets.

3. Radiation Processes

The Russian physicist Shklovsky and others realised quite early on that the observed radio emission from these sources is due to synchrotron emission, which arises when ultrarelativistic particles are accelerated in a magnetic field due to the Lorentz force. The acceleration experienced by an electron moving in a magnetic field of induction \mathbf{B} is given by:

$$\dot{\mathbf{v}} = \frac{ec}{E} \mathbf{v} \times \mathbf{B},$$

where E is the total energy of the electron. In the non-relativistic case ($\mathbf{v} \ll c$), the electron would radiate at the cyclotron frequency $\nu_c = eB_{\perp}/2\pi m_e c$, where m_e is the rest mass of the electron, and $B_{\perp} = B \sin \phi$ where ϕ is the angle between \mathbf{v} and \mathbf{B} . This gives $\nu_c \sim 2.80$ MHz per Gauss. For a typical magnetic field of

The Russian physicist Shklovsky and others realised quite early on that the observed radio emission from these sources is due to synchrotron radiation.



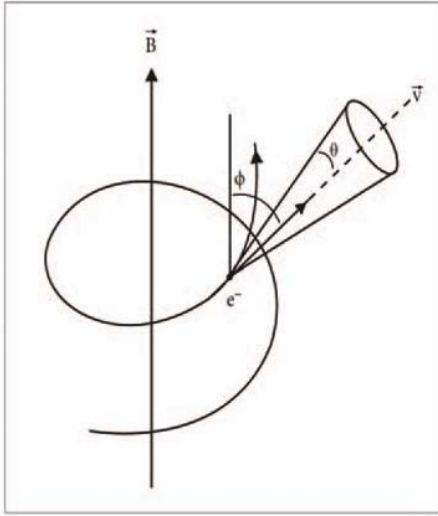


Figure 2. An ultra-relativistic electron spiraling along a magnetic field radiates synchrotron emission along the narrow cone.

say $10 \mu\text{G}$ in the lobes of a radio source, the radiation frequency would be $\sim 28 \text{ Hz}$, which would not penetrate our ionosphere, which only allows radiation above $\sim 10 \text{ MHz}$ to get through. Cyclotron emission could be observed from objects with strong magnetic fields such as the Sun and pulsars.

For a highly-relativistic electron, $v \sim c$, the gyration frequency, ν_g would be reduced because of the increased effective mass of the electron, $\nu_g = \nu_c/\gamma$. Although it might seem difficult to observe synchrotron radiation, this is not the case. With the electron moving at relativistic speeds transformations have to be made from the rest frame of the electron to that of the distant observer. This compresses the forward lobe of emission into a narrow cone with a half angle $\theta = 1/\gamma$ (Figure 2). A distant observer would see pulses of emission when the cone sweeps his/her line of sight at the Doppler shifted gyration frequency ν'_g , yielding a spectrum at all harmonics of ν'_g . For an electron with $\gamma = 10^4$ radiating in a $10 \mu\text{G}$ field with $\phi = 60^\circ$, $\nu'_g = 3.7 \times 10^{-9} \text{ MHz}$; the harmonics are closely spaced yielding a continuum. The maximum frequency seen by the observer is set by the pulse width and is given by:

$$\nu_{crit} = \frac{3e}{4\pi m_e c} \gamma^2 B_{\perp}$$



which gives a critical frequency in MHz of $4.2\gamma^2$ per Gauss. Most energy is emitted at $\nu_{max} = 0.29\nu_{crit}$. Thus an electron with $\gamma = 10^4$ ($v = 0.999999995 c$) moving in a magnetic field of $10 \mu\text{G}$ with a pitch angle of 60° would have a value of ν_{crit} of $\sim 3.6 \text{ GHz}$ and $\nu_{max} \sim 1.1 \text{ GHz}$. This is clearly observable. A power-law distribution in the energy of the radiating particles, $n(E) = n_0 E^{-\Gamma}$ would lead to an observed power-law in the observed spectrum of the source, $S(\nu) \propto \nu^{-\alpha}$, where S is the observed flux density usually expressed in units of Jansky (Jy)³, ν is the radio frequency of the observations and α defined as the spectral index is equal to $(\Gamma - 1)/2$.

The extended radio jets and lobes are optically thin, i.e., the radio emission is not absorbed either within or outside the emitting regions and have typical values of spectral indices of ~ 0.6 to 0.8 for the jets and ~ 0.8 to 1.2 for the lobes. In the compact components such as the nuclear cores, the emission could be absorbed (optically thick) and the spectra are often flat ($\alpha \sim 0$), inverted (negative values of α) or have complex shapes.

Synchrotron radiation is linearly polarized, with the degree of polarization in the extended lobes sometimes having values of about 70 per cent. However, the degree of polarization would fall if the emission is depolarized. This could happen if either the magnetic field lines in the source are very tangled, or the radiation passes through a magneto-ionic medium which rotates the electric vector of the incoming radiation (Faraday rotation) by different amounts along different lines of sight. The amount of rotation is given by $\lambda^2 \int n_e B_{\parallel} dl$, where λ is the wavelength of observations, n_e the electron density, and B_{\parallel} the component of the magnetic field parallel to the line-of-sight in the magneto-ionic medium. The integration is over the path length along the line-of-sight. Averaging the differently rotated electric vectors within the resolution beam of a telescope leads to a reduction in the degree of polarization. The degree of polarization of the nuclear radio components is usually less than a few per cent.

The total energy in the lobes of radio emission $U_{tot} = U_{par} + U_B$, sum of the energy in the cosmic ray particles, including the radi-

³ 1 Jy = $10^{-26} \text{ W Hz}^{-1} \text{ m}^{-2}$

Synchrotron radiation is linearly polarized, with the degree of polarization in the extended lobes sometimes having values of about 70 per cent. However, the degree of polarization would fall if the emission is depolarized.



ating electrons and heavier particles, and magnetic field. The energy in the magnetic field increases with B ($= B^2/8\pi$) while those in the particles decreases with magnetic field as the radiating particles lose energy faster in a higher magnetic field ($\propto B_{\perp}^2 E^2$). Therefore, the total energy U_{tot} plotted against B has a minimum value which is close to when there is equipartition between the energy in cosmic ray particles and magnetic field. The total minimum energy in the extended lobes of radio emission supplied by the jets is typically $\sim 10^{60}$ ergs.

In the context of jets, another important radiation process is inverse Compton scattering. In the familiar Compton scattering, high-energy photons scatter from free electrons imparting energy to the electrons. In inverse Compton (iC) scattering, high-energy electrons scatter off low-energy photons with the electrons losing energy while the photons gain energy. A photon of frequency ν after inverse-Compton scattering with a relativistic electron of energy $E = \gamma m_e c^2$ has a frequency ν_{iC} given by:

$$\nu_{iC} \approx \gamma^2 \nu,$$

when ($h\nu \ll m_e c^2$). A radio photon at a frequency of say 1 GHz would be scattered to a frequency of $\sim 10^{17}$ Hz via iC scattering with a relativistic electron with a Lorentz factor, γ , of 10^4 . The spectrum of the inverse-Compton radiation depends strongly on the energy distribution of the scattering electrons, and the scattered radiation has a power-law with a similar spectral index as that of the synchrotron radiation. The relativistic electrons can lose energy via both inverse-Compton and synchrotron radiation, and in an optically thin source the ratio of respective luminosities is given by the ratio of the photon and magnetic field energy densities,

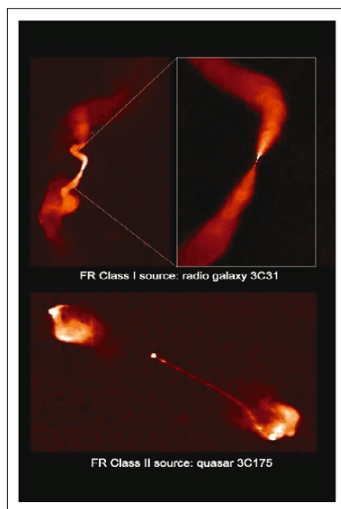
$$L_{iC}/L_s = u_{ph}/u_m.$$

The iC losses would dominate when the photon energy density exceeds the magnetic energy density. The photons could be gen-

In inverse Compton scattering, high-energy electrons scatter off low-energy photons with the electrons losing energy while the photons gain energy.



Figure 3. Radio images of the FRI radio galaxy 3C31 and the FRII radio source 3C175 associated with a quasar (Image courtesy: NRAO/AUI; <http://images.nrao.edu/AGN/>; collage from Alan Bridle's talk <http://www.cv.nrao.edu/abridle/bgctalk>; Image by Laing, Bridle, Perley, Feretti, Giovannini and Parma for 3C31, and Bridle, Hough, Lonsdale, Burns and Laing for 3C175).



erated by the synchrotron process itself, or be from the cosmic microwave background radiation.

4. Jets at Radio Wavelengths

Historically, radio sources were seen as either those dominated by the optically-thin extended lobe emission, which were more easily seen in low-frequency (< 1 GHz) surveys, and those dominated by the nuclear or core emission with flat and complex spectra, which dominate the high-frequency surveys.

The extended structure of lobe-dominated radio sources can be broadly classified into two categories: Fanaroff–Riley I and II (FRI and FRII). The FRI sources are of lower radio luminosity, have radio jets which expand into diffuse plumes or lobes of emission as the source expands into the interstellar or intergalactic medium (*Figures 3 and 4*). These jets are believed to be more dissipative than those in FRII sources, entrain material from the surrounding medium, and slow down as they advance outwards. The FRII sources are of higher luminosity, have narrow, well-collimated jets which terminate in the hotspots at the outer edges of the lobes, are less dissipative and are hence effi-



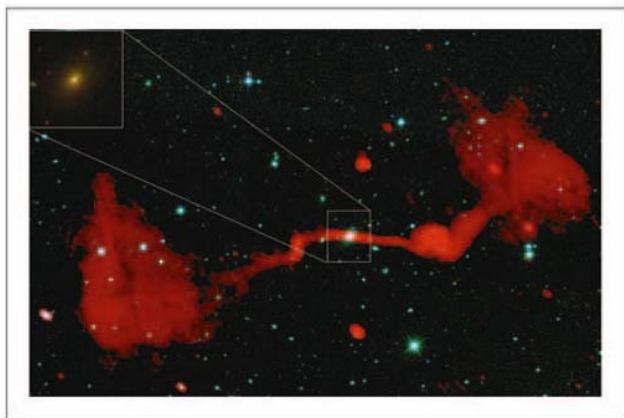


Figure 4. Radio image of a giant radio galaxy obtained with the Giant Metre-wave Radio Telescope showing the twin jets in the opposite directions, connecting the nucleus to the diffuse outer lobes of emission. (Image courtesy: Pratik Dabhade from Dabhade *et al.*, 2018, in preparation)

cient transporters of energy from the nucleus to the outer lobes. On kpc-scales, the radio jets in FRI sources tend to be more symmetric although they could be asymmetric on pc-scales close to the nucleus, while radio jets in FRII sources are often one-sided or highly asymmetric on kpc scales as well.

The nuclear or radio core components which appear as unresolved or point sources with resolutions of about an arcsec (8.1 kpc at a redshift of 1) also often reveal a core-jet structure when observed with milli-arcsec resolution. When an extended source is imaged over a large range of length scales, the nuclear jet tends to point in a similar direction as that of the larger-scale jet.

4.1 *Why are the jets one-sided?*

The sources with one-sided or highly-asymmetric jets have outer oppositely-directed lobes which are reasonably symmetric in both brightness and location. It is natural to enquire how this could arise while the jets carrying plasma from the nucleus appear to be one-sided. Although different possibilities were explored, the answer lies in the relativistic motion of the jets which boosts the flux density of the approaching jet and diminishes that of the receding one due to Doppler effects, so that the observed flux density is given by:

When an extended source is imaged over a large range of length scales, the nuclear jet tends to point in a similar direction as that of the larger-scale jet.



$$S_{obs}(\nu) = \frac{S_{int}(\nu)}{[\gamma_j(1 \pm \beta_j \cos \phi)]^{2+\alpha}},$$

where – and + refer to the approaching and receding components respectively. The ratio of flux densities of the approaching and receding components of emission, R_s , is therefore given by:

$$R_s = [(1 + \beta_j \cos \phi)/(1 - \beta_j \cos \phi)]^{2+\alpha},$$

where $v_{jet} = \beta_j c$ is the velocity of the jet. Here ϕ is the angle of inclination of the jet axis to the line of sight, and α is the spectral index of emission. For jets with a typical spectral index of 0.7, traversing outwards with a velocity of say $\sim 0.8c$ at an angle of 30° to the line-of-sight, the ratio is ~ 100 . This increases to ~ 360 when the angle of inclination decreases to 5° . Similar values are usually adequate to understand the asymmetry of most radio jets. Higher velocities and smaller angles of inclination lead to more asymmetric jets, while lower velocities and larger angles of inclination would yield more symmetric ones.

The radio sources expand and grow in size as the jets plough their way through the external medium.

The radio sources expand and grow in size as the jets plough their way through the external medium. In the FR II radio sources, the hotspots located usually at the outer extremities of the lobes are identified with the regions where the beams interact with the external medium. The lobes are formed by back flow of plasma from the hotspots. In FRI sources, where the jets are not well collimated, these expand to form diffuse plumes of emission. The hotspots and the outer lobes appear reasonably symmetric even when the jets appear one-sided in the FR II sources because of significantly smaller velocities of advancement, typically $\lesssim 0.1c$. This would imply the ratio R_s to be $\lesssim 1.7$ for a source inclined at 5° to the line-of-sight. The symmetry of the large-scale jets in the lower-luminosity FRI radio galaxies could also be attributed to smaller velocities.



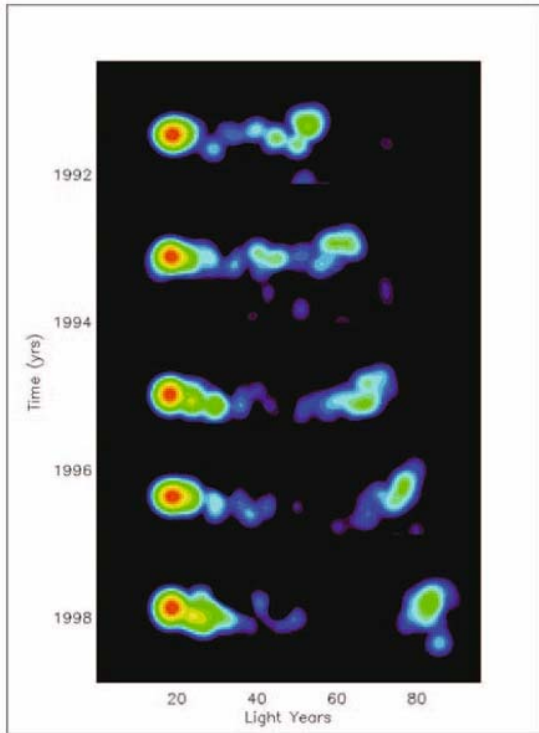


Figure 5. Superluminal motion in the core-dominated quasar 3C279. The collage of five images shown here are from a larger set of images obtained with the Very Long Baseline Array and other telescopes by Wehrle and her collaborators. The bright red spot is the stationary core, and the blue-green spot on the extreme right is part of a jet that is moving almost towards us at nearly the speed of light giving rise to apparent velocities greater than that of light (Image by Glenn Piner, Image courtesy: NRAO/AUI; <http://images.nrao.edu/387>).

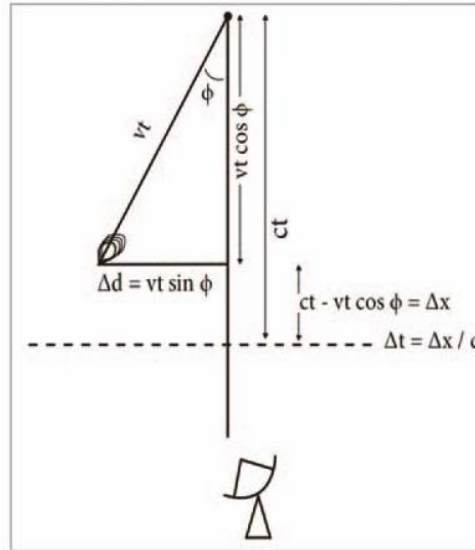
4.2 Superluminal Motion

While it is usually difficult to monitor the motion of knots or similar features in the large-scale jets because their sizes are much larger than the expected displacements which are in milli-arcsec scales, this has been now routinely done for the nuclear jets. The high-angular resolution is achieved by the techniques of very long baseline interferometry (VLBI) where the signals are combined from distant antennas, giving baselines which are often over thousands of km.

Monitoring the motion of knots or compact features in the nuclear VLBI-scale jets yielded velocities greater than that of light, first recognized in the 1970s and termed superluminal motion (*Figure 5*). Although this was initially met with scepticism, this too could be understood in terms of jets traversing at velocities close to that of light at small angles to the line of sight. The observed apparent



Figure 6. Illustration of superluminal motion where the apparent velocity of the knot travelling towards the observer $v_{app} = \beta_{app}c$ is given by $\Delta d/\Delta t$.



velocity of the compact feature in the jet, $v_{app} = \beta_{app}c$, can be expressed as:

$$\beta_{app} = \frac{\beta \sin \phi}{(1 - \beta \cos \phi)},$$

where $v = \beta c$ is the intrinsic velocity of the knot in the jet and ϕ is the angle of inclination of the jet axis to the line of sight (Figure 6). The compact knot traversing at speeds close to that of light almost keeps up with the radiation emitted earlier leading to apparent velocities greater than that of light. For example for $v = 0.99c$ and $\phi = 5^\circ$, $\beta_{app} = 6.3$. For sources inclined at small angles to the line of sight and moving at relativistic velocities, the flux density will also appear boosted. Assuming a spectral index of 0.7 for this component, the observed flux density will be boosted by a factor of ~ 530 .

5. Unified Schemes

The compact nuclear or core radio components are optically thick and have an overall flat and/or complex radio spectra caused by



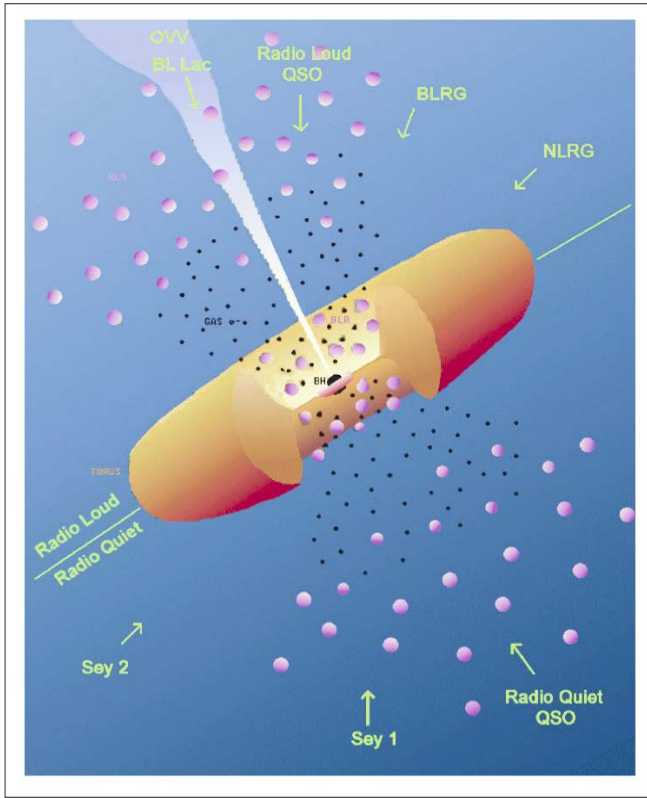


Figure 7. A schematic representation of the unified models for AGN adapted from Urry and Padovani (1995). Type I objects where the broad emission-line region is directly visible are inclined at smaller angles to the line of sight than the Type II objects, where the narrow emission lines are seen, but the broad line regions are obscured from view by the dusty torus. The width of the emission lines is due to velocities of the line-emitting clouds. The broad-line region is closer to the SMBH and the line-widths correspond to velocities of thousands of km s^{-1} , while those of the narrow-line region are usually within about hundreds of km s^{-1} . (Image reproduced courtesy: Paolo Padovani)

a combination of the spectra of the different components seen when observed with milli-arcsec resolution. When the jets in these sources are pointed at small angles to our line of sight, the flux density in these sources is boosted, giving the appearance of a core-dominated source with an overall flat/complex spectrum. These sources tend to exhibit superluminal motion, strong variability, as small intrinsic changes in either flux density or orientation can lead to large changes in the observed flux density, and one-sided or highly asymmetric radio jets. As the angle of inclination increases, the core prominence decreases and are less variable, and the jets too are weaker and less asymmetric. At large angles, the sources then appear to be dominated by the extended lobes of radio emission and have weak radio cores.

Thus, apparently different kinds of sources can be understood as



Apparently different kinds of sources can be understood as being intrinsically similar but appearing to be different because of effects of orientation and bulk relativistic motion.

being intrinsically similar but appearing to be different because of effects of orientation and bulk relativistic motion. Clearly, in such cases, properties or parameters which do not depend on orientation should be similar for the different kinds of sources. Attempts to understand apparently different kinds of AGN in such a framework are referred to as ‘unified schemes’. They reduce the apparent diversity of AGN and have had a reasonable degree of success in explaining a range of observed phenomena.

In this article, we briefly illustrate this with one such scheme, namely high-luminosity radio galaxies and quasars, which have an FR II radio structure. The properties must be consistent not merely at radio wavelengths but across the electromagnetic spectrum. *Figure 7* shows the canonical model of an AGN powered by a supermassive black hole, a broad emission-line region closer to the black hole caused by large bulk velocities of the line-emitting clouds, a narrow-line region on scales of kpc, along with a medusa shaped torus. The relative prominence and variability of the radio cores, detection of superluminal motion, and observed asymmetry of the jets can be understood if the quasars are inclined at small angles to the line of sight, and the radio galaxies at larger angles. This would be consistent with the detection of broad emission lines in quasars as we get a direct view of the nuclear region, unlike in the case of radio galaxies where usually the weaker narrow-emission lines are seen. Here, a view of the broad lines is hidden from our sight by the torus. The dividing line between the radio-loud quasars and radio galaxies has been suggested to be about 45° (the radio-loud part of *Figure 7*). Similar schemes have been suggested for radio sources with FR I radio structure and also for different types of Seyfert galaxies which are associated with spiral galaxies (the radio-quiet part of *Figure 7*) and are of much lower radio luminosity than radio galaxies and quasars. The Seyfert 1 galaxies with a direct view of the broad-line region have both broad and narrow emission lines, while in Seyfert 2 galaxies, only narrow lines are seen as the broad lines are hidden from view by the torus.

The relative prominence and variability of the radio cores, detection of superluminal motion, and observed asymmetry of the jets can be understood if the quasars are inclined at small angles to the line of sight, and the radio galaxies at larger angles.



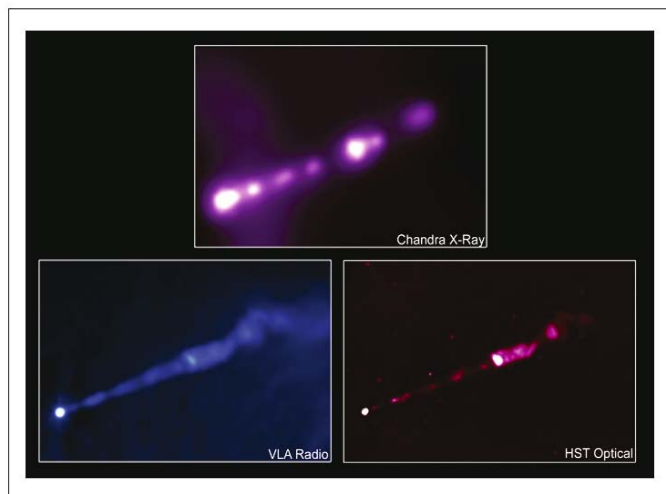


Figure 8. The jet in the nearby radio galaxy M87 as seen at X-ray, radio and optical wavelengths. The bright spot on the extreme left is the nucleus of the galaxy harbouring a supermassive black hole. The jet has several knots seen at the different wavelengths, where energy at the different wavelengths is due to synchrotron radiation. 4/ Credit:

X-ray: NASA/CXC/MIT/Marshall *et al.*, Radio: Zhou, Owen (NRAO), Biretta (STScI); Optical: NASA/STScI/UMBC/Perlman *et al.*)

6. Jets at X-ray Wavelengths

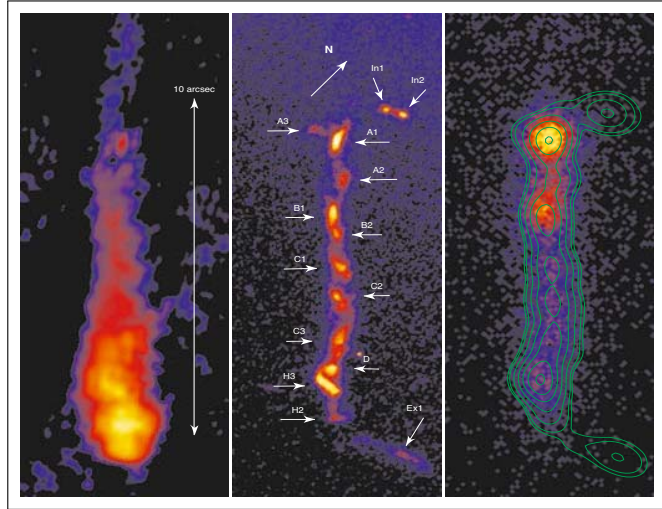
The launching of the Chandra X-ray observatory and the serendipitous discovery of an X-ray jet associated with the radio jet of the quasar PKS0637–752, heralded the beginning of a new dimension to the study of radio jets. More than a hundred radio-loud AGN⁴ have been shown to have X-ray counterparts of radio emission from either the jets, hot-spots or lobes on length scales from tens to hundreds of kpc.

The jets exhibit a wide variety in their radio and X-ray emission (*Figures 8 and 9*). For example, in the nearby FRI radio galaxy M87 (Virgo A) almost all the knots or peaks of emission have been detected in the X-rays. The spectral energy distribution of emission from these features from radio through optical to X-rays can be understood as being due to synchrotron radiation from a single electron population. However, in the case of X-ray knots in jets in quasars, the spectra appear harder and cannot be understood as an extension of the synchrotron spectrum. In these situations, the X-ray emission could be due to inverse Compton scattering with either the synchrotron photons referred to as synchrotron self-Compton or SSC, or those of the cosmic

⁴<https://hea-www.harvard.edu/XJET/>



Figure 9. The jet in the quasar 3C273 at radio, optical and X-ray wavelengths (from left to right) as seen with MERLIN of the Jodrell Bank Observatory, Hubble Space Telescope and Chandra X-ray Observatory respectively. The overlaid contours in the right panel are a smoothed version of the optical image in the centre, showing a pretty good match, except for the two unrelated features near the top and one in the bottom. The jet originates in the quasar nucleus which is beyond the top of the image. The scale of the image is about 10 arcsec in all three images. (Image courtesy Herman Marshall; and <http://chandra.harvard.edu/photo/2000/0131/more.html>; Credit: Radio: MERLIN; Optical: NASA/STScI; X-ray: NASA/CXC))



microwave background radiation, referred to as external Compton or EC. The more favoured explanation for these jets moving at relativistic speeds is inverse Compton scattering with the CMB radiation whose energy density increases by the square of the bulk Lorentz factor in the rest frame of the jet. The energy density of the CMB photons increases with redshift, z , as $(1+z)^4$, making the process more effective at high redshifts. Estimates based on this model for a sample of quasar jets yield bulk Lorentz factors of ~ 10 and magnetic field strengths of $\sim 10 - 20 \mu\text{G}$.

7. Concluding Remarks

There has been significant progress in our understanding of jets from multi-wavelength, high-resolution observations over the last several decades. However, there are a number of aspects that are not well understood. For example, in a sample of elliptical galaxies, all harbouring supermassive black holes in their nuclear regions, only about 10 per cent are luminous at radio frequencies producing prominent jets and lobes. This dichotomy between these radio-loud AGNs and the radio-quiet ones remains unclear. The radio-quiet ones are weaker in luminosity by about a couple of orders of magnitude on average and may also show evidence of collimated outflows or jets but of much lower luminosity. Galax-

ies classified as starburst galaxies or those with low-ionization nuclear emission-line regions (LINERs) are also known to have collimated structures or jets, suggesting that AGN and starburst phenomena co-exist. The relationship between these two forms of activity, the detailed physics of the launching of jets from an SMBH/accretion disk system, and the precise composition of the jets continue to be challenging and interesting areas of research.

Acknowledgments

The author wishes to thank Preeti Kharb, Dharam Vir Lal, and Biman Nath for their comments on an earlier version of the manuscript.

Suggested Reading

- [1] J A Irwin, *Astrophysics Decoding the Cosmos*, Wiley, 2007.
- [2] K I Kellermann, F N Owen, *Radio Galaxies and Quasars, in Galactic and Extragalactic Radio Astronomy*, eds G L Verschuur, K I Kellermann, Springer-Verlag, 1974.
- [3] A K Kembhavi, J V Narlikar, *Quasars and Active Galactic Nuclei*, Cambridge University Press, 1999.
- [4] M S Longair, *High Energy Astrophysics*, Cambridge University Press, 2011.
- [5] A T Moffet, Strong Nonthermal Radio Emission from Galaxies, in *Stars and Stellar Systems, Vol.IX, Galaxies and the Universe*, eds A Sandage, M Sandage, J Kristian, The University of Chicago Press, p.211, 1975.

Address for Correspondence
D J Saikia
National Centre for Radio
Astrophysics
Tata Institute of Fundamental
Research
Pune University Campus
Post Bag 3, Ganeshkhind
Pune 411 007, India.
Email:
djs@ncra.tifr.res.in

